Macromolecular Research, Vol. 16, No. 2, pp 113-119 (2008)

Thermal and Solid State Assembly Behavior of Amphiphilic Aliphatic Polyether Dendrons with Octadecyl Peripheries

Yeon-Wook Chung, Byung-Ill Lee, and Byoung-Ki Cho*

Department of Chemistry and Institute of Nanosensor and Biotechnology, Dankook University, Gyeonggi-do 448-701, Korea

Received July 30, 2007; Revised November 5, 2007

Abstract: A series of amphiphilic dendrons **n-18** (**n**: generation number, **18**: octadecyl chain) based on an aliphatic polyether denderitic core and octadecyl peripheries were synthesized using a convergent dendron synthesis consisting of a Williamson etherification and hydroboration/oxidation reactions. This study investigated their thermal and self-assembling behavior in the solid state using differential scanning calorimetry (DSC), Fourier transform infrared (FT-IR) absorption spectroscopy, and small angle X-ray scattering (SAXS). DSC indicated that the melting transition and the corresponding heat of the fusion of the octadecyl chain decreased with each generation. FT-IR showed that the hydroxyl focal groups were hydrogen-bonded with one another in the solid state. DSC and FT-IR indicated microphase-separation between the hydrophilic dendritic cores and hydrophobic octadecyl peripheries. SAXS data analysis in the solid state suggested that the lower-generation dendrons **1-18** and **2-18** self-assemble into lamellar structures based upon a bilayered packing of octadecyl peripheries. In contrast, the analyzed data of higher-generation dendron **3-18** is consistent with 2-D oblique columnar structures, which presumably consist of elliptical cross sections. The data obtained could be rationalized by microphase-separation between the hydrophilic dendritic core and hydrophobic octadecyl peripheries, and the degree of interfacial curvature associated with dendron generation.

Keywords: amphiphilic, dendrons, thermal property, solid state assembly.

Introduction

Molecularly uniform dendron molecules, i.e. parts of dendrimers with symmetric shapes, have been attractive as organic molecular building blocks due to their well-defined molecular weights and fanwise shapes.[1] Particularly, chemical modifications of conformationally-distinct branched dendritic core and linear peripheral groups can reinforce microphase-separation in the core-shell architecture, resulting in self-assembled nanostructures.[2] For example, rigid aromatic benzyl-unit-based dendritic cores combined with flexible alkyl peripheries have produced liquid crystalline dendron molecules that are organized into ordered structures in the melt. In these molecules, supramolecular assemblies have been systematically modulated from lamellar, tubular, columnar up to various micellar phases via molecular engineering of the generation, focal group and number/site of peripheral groups on aromatic units.[3]

In addition to rigid poly(benzyl ether) dendrons, dendrons with aliphatic cores such as poly(amidoamine) (PAMAM) and poly(propyleneimine) (PPI) have been employed for the study of self-assembly behavior in the bulk state.[4] However, these aliphatic amine dendrons have needed special chemical treatments, e.g., the introduction of hydrophilic carboxylic acid end peripheries or protonation of amine dendritic cores, to induce microphase-separated nanostructures.[4a,b] In this regard, a more hydrophilic aliphatic polyether dendritic structure devised by Fréchet *et al*. was suggested as an ideal candidate to prepare amphiphilic dendrons,[5] because the repeat unit of $CH_2CH(CH_2O)_2$ is almost comparable to that of poly(ethylene oxide), which is one of the most hydrophilic polymers. Recently, Cho *et al*. synthesized dendrons from first to fourth generations using the aliphatic polyether dendritic core and hydrophobic crystalline docosyl peripheries, and investigated their solid state assembly behavior as a function of generation.[6] The researchers observed that all the dendrons exhibited microphase-separated nanostructures, which are lamellar and columnar structures for first through third and fourth generations, respectively.

As an extension of the above work, we examined thermal and assembling behavior in the solid state of amphiphilic aliphatic polyether dendrons with shorter alkyl chain, i.e., octadecyl chain. In this paper, we address the synthesis of the dendron molecules (**n-18**) and the characterization of

*Corresponding Author. E-mail: chobk@dankook.ac.kr

their physical properties using differential scanning calorimetry (DSC), infrared spectroscopy (IR) and small angle X-ray scattering (SAXS) experiments.

Experimental

Characterization. ^{1}H-NMR spectra were recorded from $CDCl_3$ solutions on a Varian 200 spectrometer. The purity of the products was checked by thin-layer chromatography (TLC; Merck, silica gel 60). A Perkin Elmer Pyris Diamond differential scanning calorimeter equipped with a model 1020 thermal analysis controller was used to determine thermal transitions, which were reported as the maxima and minima of their endothermic or exothermic peaks. In all cases, heating and cooling scans were measured at a rate of 10 °C/min. Gel permeation chromatography (GPC) measurements were conducted in tetrahydrofuran (THF) using a Waters R401 instrument equipped with Stragel HR 2, 3 and 4 columns at a flow rate of 1.0 mL/min. X-ray scattering measurements were performed in transmission mode with synchrotron radiation at the 10C1 X-ray beam line of the Pohang Accelerator Laboratory, Korea. The sample was held in an aluminum sample holder with films on both sides. MALDI-TOF mass spectra were performed on a Perceptive Biosystems Voyager-DE STR system using a 2,5-dihydroxy benzoic acid matrix. Microanalyses were performed with a Perkin Elmer 240 elemental analyzer at the Organic Chemistry Research Center, Sogang University, Korea. The compounds were purified by column chromatography (silica gel) and prep-HPLC (Japan Analytical Instrument).

Synthesis. Synthesis of dendrons **n-18** with a hydroxyl focal group (here, **n** and **18** designate the dendron generation and octadecyl chain, respectively) were performed on a convergent synthetic route consisting of a Williamson etherification and hydroboration/oxidation reactions, as outlined in Scheme I.[5] Olefin precursors of hydroxyl-terminated dendrons are denoted by adding suffix "–ene".

Synthesis of 1-18-ene. 1-Octadecanol (135.2 g, 500 mmol), NaH (26.2 g 600 mmol), and methallyl dichloride (25.0 g, 200 mmol) were dissolved in 600 mL of a THF/DMF solvent mixture. The mixture was heated at reflux for 57 h under N_2 atmosphere and then quenched with water. After cooling to room temperature, THF was removed in a rotary evaporator. The mixture was poured into methyl alcohol. The precipitate was collected using a glass filter and removed dark-brown color through a column of silica gel with chloroform as an eluent. The obtained compound was purified by several recrystallizations from *n*-hexane:ethyl acetate = 1:3 solvent mixture to yield 87 g (73%) of a white crystal. ^{1}H-NMR ($CDCl_3$, δ, ppm): 5.16 (s, 2H), 3.96 (s, 4H), 3.40 (t, 4H, J = 6.6 Hz), 1.25-1.56(m, 64H), 0.88 (t, 6H, J = 6.4 Hz); M_w/M_n = 1.01 (GPC).

Synthesis of 1-18. 1-18-ene (85.0 g, 143 mmol) was dissolved in 918 mL of 0.5 M of 9-BBN solution in THF under a N_2 atmosphere at room temperature. The reaction mixture was stirred for 22 h at 35 °C, then carefully quenched with 190 mL of 3 M NaOH aqueous solution, and then stirred for 90 min at room temperature. 190 mL of 30% H_2O_2 aqueous solution was carefully added. The mixture was stirred for 1 h at room temperature, and THF was then removed in a rotary evaporator. The mixture was saturated with K_2CO_3 and extracted with chloroform. After removing chloroform in a rotary evaporator, the resulting solid was purified by several recrystallizations from ethyl acetate to yield 75 g (85%) of a white solid. ^{1}H-NMR ($CDCl_3$, δ, ppm): 3.76 (t, 2H), 3.56 (m, 4H), 3.41 (t, 4H, J = 6.6 Hz), 2.85 (t, 1H), 2.10 (m, 1H), 1.26-1.55 (m, 64H), 0.88 (t, 6H, J = 6.3 Hz). MS (MALDI-TOF): m/z calcd for ($C_{40}H_{82}O_3$) 610.63; found 610.69. Anal. Calcd for $C_{40}H_{82}O_3$: C, 78.62; H, 13.53. Found: C, 78.66; H, 13.58; M_w/M_n = 1.01 (GPC).

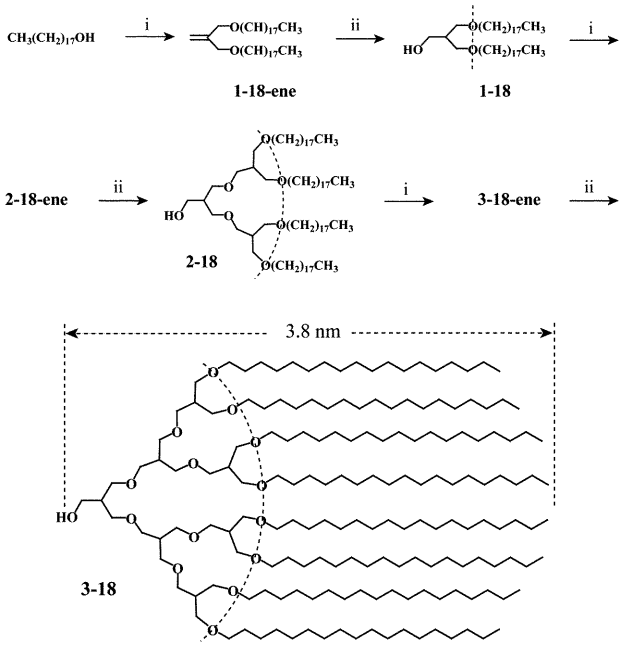

Scheme I. Synthesis of amphiphilic dendrons **1-18**, **2-18** and **3-18**; i) NaH, methallyl dichloride, ii) (1) 9-BBN, (2) H_2O_2/NaOH. The dotted line in the molecular structures indicates the intrinsic curvature, which increases when going to a higher generation.

Synthesis of 2-18-ene. 1-18 (60.0 g 98 mmol), NaH (5.2 g 120 mmol), and methallyl dichloride (5.6 g, 44 mmol) were dissolved in 360 mL of a THF/DMF solvent mixture. The mixture was heated at reflux for 51 h under N_2 atmosphere and then quenched with water. After cooling to room temperature, THF was removed in a rotary evaporator. The mixture was poured into methyl alcohol. The precipitate was collected using a glass filter and removed dark-brown color through a column of silica gel with chloroform as an eluent. The obtained compound was purified by several

recrystallizations from *n*-hexane:ethyl acetate = 1:3 solvent mixture to yield 50.0 g (88%) of a white crystal. ^{1}H-NMR ($CDCl_3$, δ, ppm): 5.14 (s, 2H), 3.94 (s, 4H), 3.48-3.46 (m, 20H), 2.15 (m, 2H), 1.25-1.56 (m, 128H), 0.88 (t, 12H, J= 6.1 Hz); M_w/M_n = 1.01 (GPC).

Synthesis of 2-18. 2-18-ene (52.0 g, 48 mmol) was dissolved in 244 mL of 0.5 M of 9-BBN solution in THF under a N_2 atmosphere at room temperature. The reaction mixture was stirred for 24 h at 35 °C, then carefully quenched with 54.4 mL of 3 M NaOH aqueous solution, and then stirred for 1 h at room temperature. Approximately 54.4 mL of 30% H_2O_2 aqueous solution was carefully added. The mixture was stirred for 1 h at room temperature, and THF was then removed in a rotary evaporator. The mixture was saturated with K_2CO_3 and extracted with chloroform. After removing chloroform in a rotary evaporator, the resulting solid was purified by several recrystallizations from ethyl acetate to yield 42 g (79.6%) of a white solid. ^{1}H-NMR ($CDCl_3$, δ, ppm): 3.73 (t, 2H), 3.34-3.51 (m, 24H), 2.87 (t, 1H) 2.13 (m, 3H), 1.25-1.55 (m, 128H), 0.88 (t, 12H, J = 6.3 Hz). MS (MALDI-TOF): m/z calcd for ($C_{84}H_{170}O_7$) 1291.29; found 1291.46. Anal. Calcd for $C_{84}H_{170}O_7$: C, 78.07; H, 13.26. Found: C, 78.06; H, 13.13; M_w/M_n = 1.01 (GPC).

Synthesis of 3-18-ene. **2-18** (45.0 g, 38.7 mmol), NaH (1.8 g 41.5 mmol), and methallyl dichloride (2.1 g, 18.9 mmol) were dissolved in 200 mL of a THF/DMF solvent mixture. The mixture was heated at reflux for 48 h under N_2 atmosphere and then quenched with water. After cooling to room temperature, THF was removed in a rotary evaporator. The mixture was poured into methyl alcohol. The precipitate was collected using a glass filter and removed dark-brown color through a column of silica gel with chloroform as an eluent. The obtained compound was purified by several recrystallizations methylene chloride:ethyl acetate = 1:2 solvent mixture at -5 °C to yield 17 g (34.2%) of a white crystal. ^{1}H-NMR ($CDCl_3$, δ, ppm): 5.13 (s, 2H), 3.91 (s, 4H), 3.34-3.43 (m, 52H), 2.12 (m, 6H), 1.25-1.55 (m, 256H), 0.87 (t, 24H, J = 6.4Hz); M_w/M_n = 1.02 (GPC).

Synthesis of 3-18. 3-18-ene (17.0 g, 6.45 mmol) was dissolved in 38.7 mL of 0.5 M of 9-BBN solution in THF under a N_2 atmosphere at room temperature. The reaction mixture was stirred for 24 h at 35 °C, then carefully quenched with 8.6 mL of 3 M NaOH aqueous solution, and then stirred for 1 h at room temperature. 8.6 mL of 30% H_2O_2 aqueous solution was carefully added. The mixture was stirred for 1 h at room temperature, and THF was then removed in a rotary evaporator. The mixture was saturated with K_2CO_3 and extracted with chloroform. After removing chloroform in a rotary evaporator, the resulting solid was purified by several recrystallizations from ethyl acetate to yield 10 g (58.5%) of a white solid. ^{1}H-NMR ($CDCl_3$, δ, ppm): 3.71 (t, 2H), 3.34-3.43 (m, 56H), 2.86 (t, 1H) 2.12 (m, 7H), 1.25-1.54 (m, 256H), 0.88 (t, 24H, J = 6.4 Hz). MS (MALDI-TOF): m/z calcd for ($C_{172}H_{346}O_{15}$) 2652.63; found 2652.94. Anal. Calcd for $C_{172}H_{346}O_{15}$: C, 77.82; H, 13.14. Found: C, 77.80; H, 13.01; M_w/M_n = 1.01 (GPC).

Results and Discussion

Synthesis. Amphiphilic dendrons **n-18** consist of hydrophilic aliphatic polyether dendritic cores, hydrophobic octadecyl peripheries, and a hydroxyl focal group. To generate the aliphatic polyether cores, the repeating unit of which is almost analogous to a conventionally used hydrophilic linear segment such as poly(ethylene oxide) (PEO), we employed a convergent procedure developed by the Fréchet group (Scheme I).[5,6] The convergent synthetic route consists of Williamson etherification and hydroboration/oxidation, which are chain growth and activation steps, respectively. The growth step, the etherification of the hydroxyl terminus of octadecyl chain with methallyl dichloride, was implemented in a THF/DMF solvent mixture (3:1 volume ratio) in the presence of sodium hydride as a base. The reason for the addition of DMF is to enhance the reactivity of the deprotonated oxyanion end of the octadecyl chain because the polar aprotic solvent effectively dissociates the anion from the countercation Na^+. After the chain growth step, the olefin compounds were purified simply by recrystallization. **1-18-ene**/**2-18-ene** and **3-18-ene** were refined using *n*-hexane:ethyl acetate = 1:3 and methylene chloride:ethyl acetate = 1:2 solvent mixtures, respectively. The obtained olefin precursors were then activated into alcohol products through hydroboration/oxidation reactions. To eliminate an undesirable *tert*-alcoholic isomer, sterically hindered 9-BBN was used as the hydroboration reagent. During the reaction, reaction vessels were warmed at 35 °C, because **1-18-ene** and **2-18-ene** were precipitated at room temperature. Subsequently, an oxidation reaction was carried out by the insertion of NaOH/H_2O_2. Crude products were purified by repetitive recrystallization from ethyl acetate. The characterization of **n-18** was performed by ^{1}H-NMR, gel permeation chromatography (GPC), infrared spectroscopy (IR), elemental analysis, and mass spectrometry. All the dendrons show narrow polydispersities (M_w/M_n) of less than 1.02 in GPC (Figure 1). MALDI-TOF mass data display a single peak corresponding to [dendron + Na]$^+$ in the spectra of dendrons, and the calculated molecular weights from the peak positions are in good agreement with the theoretical values (Figure 2 and Table I). The analytical data confirm the successful synthesis of the dendrons in high purity.

Thermal Behavior and Microphase-Separation in Solid State. The thermal properties such as melting transitions and heats of fusion of **n-18** were characterized by differential scanning calorimetry (DSC), as summarized in Table I. As expected from the molecular shapes of the dendritic core (amorphous branched) and the octadecyl chain (crystalline linear), all the dendrons show a single peak on the heating scan, which corresponds to the melting transition of the

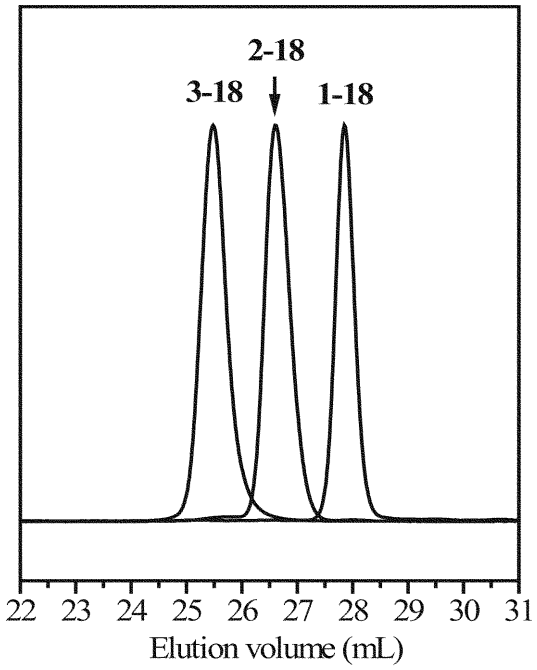

Figure 1. GPC curves of **1-18**, **2-18** and **3-18**.

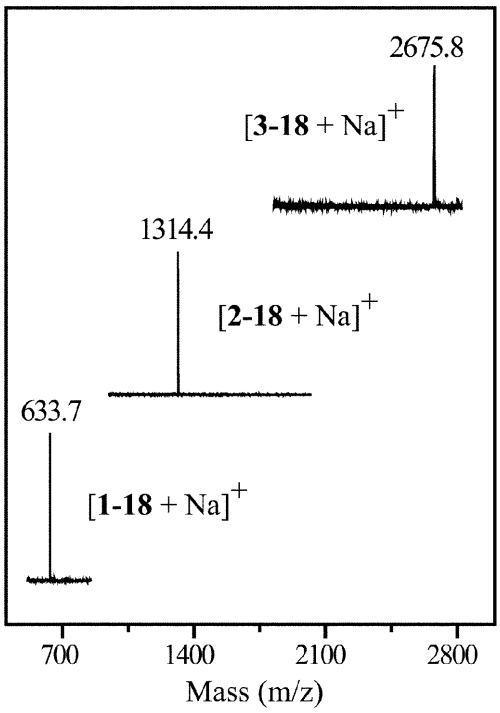

Figure 2. MALDI-TOF mass spectra of **1-18**, **2-18** and **3-18**.

crystalline octadecyl peripheries to isotropic liquid. The observed melting temperatures and the corresponding heats of fusion of dendrons decline gradually from generation to generation (Figure 3 and Table I). By comparing the experimentally determined heats of fusion to that of a perfect crystalline octadecyl chain,[7] the degree of crystallinity of the

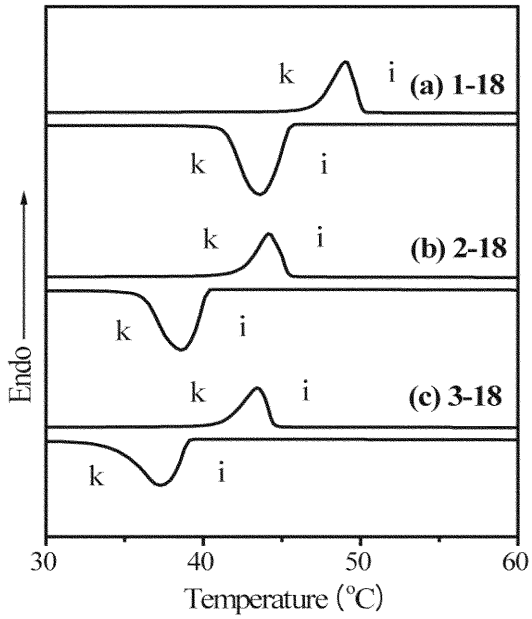

Figure 3. DSC thermograms of (a) **1-18**, (b) **2-18**, and (c) **3-18**. The endothermic and exothermic peaks were recorded during the first heating (upper curve) and cooling (lower curve) scans, respectively; k: crystalline, i: isotropic liquid phases.

octadecyl peripheries in **n-18** were calculated, and the value decreases from 49.3% to 43.1% as the generations increase. These reductions of the degree of crystallinity as well as the melting temperatures might be attributed to the intrinsic curvature associated with fanwise dendritic architecture. As represented as dotted lines in Scheme I, more curved intrinsic curvature at higher generation would cause a wavy interface rather than a flat interface when dendrons form into a crystalline structure, resulting in a less regular packing of octadecyl peripheries. The generation-dependent thermal behavior in the solid state suggests a microphase-separation between dendritic cores and octadecyl peripheries, attributable to hydrophobic and crystallization effects. If octadecyl chains were mingled with dendritic cores at the molecular level, no melting would be expected.

Meanwhile, the microphase-separation was corroborated by investigating an IR absorption signal of a stretching vibration of hydroxyl focal groups. In the solid state, translational molecular motions are restricted, while short-range segmental motions of the amorphous dendritic parts are allowed. Thus, identification of hydrogen bonding of hydroxyl focal groups may indicate that dendritic cores stand close to one another, suggesting compartmentalization of dendritic cores and alkyl chains regions. Figure 4 shows the IR spectra of **1-18**, **2-18** and **3-18**. Contrary to the non-hydrogen bonded alcohols that show a sharp absorption peak near 3600 cm^{-1}, the observed IR spectra exhibit a broad band over 3100-3600 cm^{-1}.[8] Considering the peak width as well as the frequency, the data show that hydroxyl groups are

Table I. Characterization of Amphiphilic Dendrons 1-18, 2-18, and 3-18

Amphiphilic Dendron	mol. wt. (g/mol)		Molecular Length (nm)[c]	Weight Fraction of Octadecyl Periphery *f*	Crystallinity of Octadecyl Chain (%)[d]	Melting Transitions (°C) and Corresponding Enthalpy Changes (J/g)	
	a	*b*				Heating	Cooling
1-18	610.6	610.7	2.87	0.83	49.3	k 50.9 (119.4) i k 49.0 (118.0) i	k 43.6 (118.8) i
2-18	1291.3	1291.5	3.34	0.78	45.8	k 45.9 (104.4) i k 44.1 (104.4) i	k 38.5 (104.9) i
3-18	2652.6	2652.9	3.80	0.76	43.1	k 45.1 (95.7) i k 43.9 (96.4) i	k 36.7 (90.7) i

[a]Theoretical molecular weight. [b]Determined by MALDI-TOF MS. [c]Fully stretched chain length from the focal hydroxyl group to the methyl group of octadecyl chain. [d]Degree of crystallinity = experimental heat of fusion of a single octadecyl group on the first heating/heat of fusion of a perfect crystalline octadecyl chain. Experimental heat of fusion of a single octadecyl group (kJ/mol) = heat of fusion (J/g) from first heating × mass of a single octadecyl group (253.3 g/mol)/*f*. The heat of fusion of a single perfect crystalline octadecyl group was calculated on the basis of the heat of fusion of a methylene unit in the perfect crystalline polyethylene of 4.11 kJ/mol.

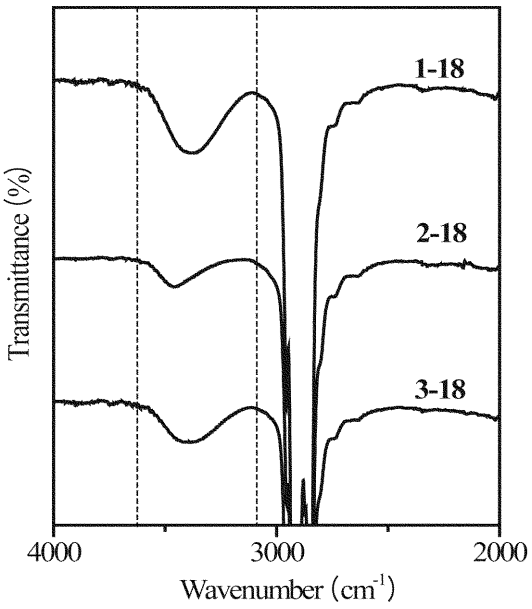

Figure 4. IR spectra of **1-18**, **2-18**, and **3-18**. The dotted region corresponds to the absorption of hydrogen-bonded O-H stretching vibration.

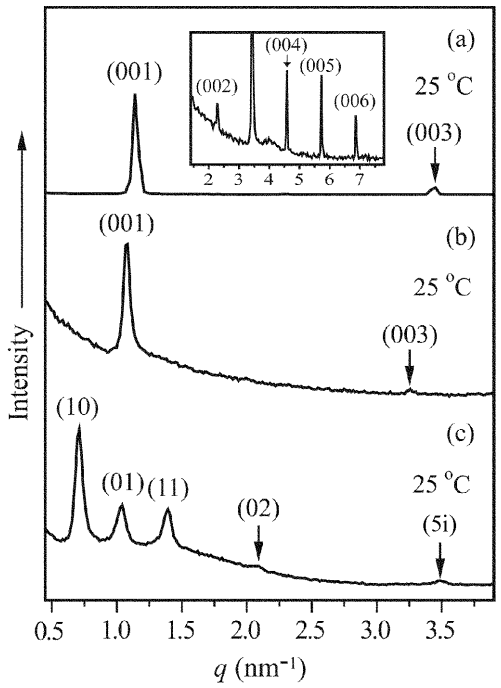

Figure 5. Small-angle X-ray scattering patterns of (a) **1-18**, (b) **2-18**, and (c) **3-18**.

hydrogen-bonded. Thus, we can speculate that hydroxyl groups are localized in microphase-separated domain structures.

Solid State Self-Assembly. As evidenced by the thermal and spectroscopic observations, we can suggest microphase-separated nanostructures are assembled by the respective generations in the solid state. Thus, it would be interesting to examine the solid state microstructures of **n-18** as a function of dendron generation. To investigate, we carried out small-angle X-ray scattering (SAXS) experiments at 25 °C. In Figure 5(a), the SAXS spectrum of **1-18** shows multiple reflections with equidistant q-spacing, which is suggestive of a lamellar structure. From the primary reflection, the lattice constant (i.e., periodic layer distance) was estimated 5.5 nm. Similarly, the SAXS pattern of **2-18** could be interpreted as a lamellar structure with a lattice constant of 5.8 nm (Figure 5(b)).

By considering the fully stretched octadecyl chain length of 2.34 nm from the Corey-Pauling-Koltun (CPK) model, in the lamellar structures octadecyl peripheries may pack in a bilayer fashion. The slight increase of the interlayer distance from **1-18** to **2-18** is because of the increased length of dendritic core edge. On the basis of the SAXS data together with the DSC and IR results, the solid state structures of **1-18** and **2-18** can be illustrated in Figure 6(a). In the middle of crystalline octadecyl bilayers, dendritic cores form amorphous layers in which hydrogen-bonded hydroxyl focal groups exist. In contrast, the SAXS spectrum of **3-18** dis-

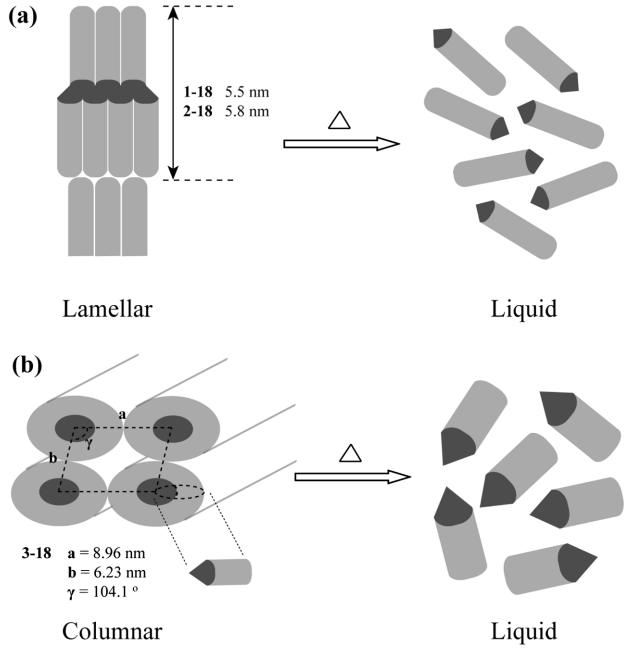

Figure 6. Schematic sketches of morphological transitions from (a) the lamellar structures of **1-18**/**2-18** and (b) oblique columnar structure of **3-18** to isotropic liquid states upon heating.

plays five well-resolved reflections with q-spacing ratios of 1.46:1.96:2.94:4.90, the pattern of which deviated from lamellar or other conventional lattices such as hexagonal/or tetragonal ones (Figure 5(c)). Compared to the SAXS data of **1-18** and **2-18**, another contrast is the primary peak position which is considerably shifted to the small-angle region. On going from **2-18** to **3-18**, the increase (3.04 nm) of primary d-spacing is greater than that (0.47 nm) of the dendritic core edge. By fitting to various structural models, the SAXS pattern was interpreted as a 2-D oblique columnar lattice consisting of columns with an elliptical cross section rather than a circular one (Figure 6(b)).[9] The lattice parameters were estimated to be a = 8.96 nm, b = 6.23 nm, and γ = 104.1°. The formation of the oblique columnar structure might be due to the crystallization of the octadecyl peripheries preferentially along the longer axis of the elliptical cross-section.[10]

As compared to the previously reported dendron system with longer docosyl peripheries,[6] a remarkable contrast in this series is that the structural transition from lamellar to columnar structures occurs between 2nd and 3rd generations. On the other hand, the dendron system with docosyl peripheries displays a similar transition on going from 3rd to 4th generations. The observed morphological transition of **n-18** in the earlier generation suggests that at a given generation dendrons with shorter crystalline alkyl peripheries adopt less anisotropic molecular sections in the solid state, thus organize to form columnar rather than lamellar assemblies. In the end, the results can rationalize the effect of crystalline peripheral chain length on the solid-state assembly of amphiphilic dendrons.

Conclusions

We synthesized amphiphilic dendrons (**n-18**) based on an aliphatic hydrophilic polyether dendritic core and hydrophobic octadecyl peripheries via a convergent method consisting of a Williamson etherification and hydroboration/oxidation reaction, and characterized their thermal and self-assembling properties using DSC, IR and SAXS. DSC and IR data suggest a microphase-separation between hydrophilic dendritic cores and hydrophobic octadecyl peripheries in the solid state. Melting transitions and the corresponding heats of fusion of octadecyl peripheries decrease slightly as a function of generation. Morphological studies of **1-18** and **2-18** indicate lamellar structures with octadecyl bilayers, while **3-18** exhibits a 2-D oblique columnar arrangement. The observed thermal and self-assembly properties can be elucidated in terms of microphase-separation between hydrophilic dendritic cores and hydrophobic octadecyl peripheries associated with hydrophobic and crystallization effects, and variation of the molecular shape in the solid state dependent upon dendron generation and peripheral chain length.

Acknowledgment. The present research was conducted by the research fund of Dankook University in 2006. We thank the Pohang Accelarator Laboratory (Beamline 10C1), Korea, for use of synchrotron radiation.

References

(1) a) A. W. Bosman, H. M. Janssen, and E. W. Meijer, *Chem. Rev.*, **99**, 1665 (1999). b) S. M. Grayson and J. M. J. Fréchet, *Chem. Rev.*, **101**, 3819 (2001). c) H. D. Hudson, H.-T. Jung, V. Percec, W.-D. Cho, G. Johansson, G. Ungar, and V. S. K. Balagurusamy, *Science*, **278**, 449 (1997). d) L. Gehringer, C. Bourgogne, D. Guillon, and B. Donnio, *J. Am. Chem. Soc.*, **126**, 3856 (2004). e) M. Fisher and F. Vögtle, *Angew. Chem. Int. Ed.*, **38**, 884 (1999). f) A. Hirao, Y. Tsunoda, A. Matsuo, K. Sugiyama, and T. Watanabe, *Macromol. Res*., **14**, 272 (2006).

(2) a) C. Park, I. H. Lee, S. Lee, Y. Song, M. Rhue, and C. Kim, *Proc. Natl. Acad. Sci. USA*, **103**, 1199 (2006). b) Y. Kamikawa and T. Kato, *Org. Lett.*, **8**, 2463 (2006). c) L. Gehringer, D. Guillon, and B. Donnio, *Macromolecules*, **36**, 5593 (2003). d) K. T. Kim, I. H. Lee, C. Park, Y. Song, and C. Kim, *Macromol. Res*., **12**, 528 (2004). e) Y. Song, C. Park, and C. Kim, *Macromol. Res*., **14**, 235 (2006).

(3) a) D. R. Dukeson, G. Ungar, V. S. K. Balagurusamy, V. Percec, G. Johansson, and M. Glodde, *J. Am. Chem. Soc.*, **125**, 15974 (2003). b) M. Suárez, J.-M. Lehn, S. C. Zimmerman, A. Skoulios, and B. Heinrich, *J. Am. Chem. Soc.*, **120**, 9526 (1998). c) V. Percec, W.-D. Cho, G. Ungar, and D. J. P. Yeardley, *J. Am. Chem. Soc.*, **123**, 1302 (2001). d) G. Ungar, Y. Liu,

X. Zeng, V. Percec, and W.-D. Cho, *Science*, **299**, 1208 (2003). e) X. Zeng, G. Ungar, Y. Liu, V. Percec, A. E. Dulcey, and J. K. Hobbs, *Nature*, **428**, 157 (2004). f) D. J. P. Yeardley, G. Ungar, V. Percec, M. N. Holerca, and G. Johansson, *J. Am. Chem. Soc.*, **122**, 1684 (2000). g) V. Percec, M. Peterca, M. J. Sienkowska, M. A. Ilies, E. Aqad, J. Smidrkal, and P. A. Heiney, *J. Am. Chem. Soc.*, **128**, 3324 (2006). h) V. Percec, A. E. Dulcey, M. Peterca, P. Adelman, R. Samant, V. S. K. Balagurusamy, and P. A. Heiney, *J. Am. Chem. Soc.*, **129**, 5992 (2007).

(4) a) J. C. M. van Hest, M. W. P. L. Baars, C. Elissen-Román, M. H. P. van Genderen, and E. W. Meijer, *Macromolecules,* **28**, 6689 (1995). b) C. Román, H. R. Fischer, and E. W. Meijer, *Macromolecules*, **32**, 5525 (1999). c) A. P. H. J. Schenning, C. Elissen-Román, J.-W. Weener, M. W. P. L. Baars, S. J. van der Gaast, and E. W. Meijer, *J. Am. Chem. Soc.*, **120**, 8199 (1998). d) J. Iyer and P. T. Hammond, *Langmuir*, **15**, 1299 (1999). e) J. Iyer, K. Fleming, and P. T. Hammond, *Macromolecules,* **31**, 8757 (1998). f) J. H. Cameron, A. Facher, G. Lattermann, and S. Diele, *Adv. Mater.*, **9**, 398 (1997).

(5) A) M. Jayaraman and J. M. J. Fréchet, *J. Am. Chem. Soc.*, **120**, 12996 (1998). b) B.-K. Cho and Y.-W. Chung, *Bull. Korean Chem. Soc.*, **27**, 29 (2006). c) Y.-S. Yoo, J.-H. Choi, J.-H. Song, N.-K. Oh, W.-Z. Zin, S. Park, T. Chang, and M. Lee, *J. Am. Chem. Soc.*, **126**, 6294 (2004).

(6) B.-K. Cho, A. Jain, J. Nieberle, S. Mahajan, U. Wiesner, S. M. Gruner, S. Türk, and H. J. Räder, *Macromolecules*, **37**, 4227 (2004).

(7) Y. L. Loo, R. A. Register, and D. H. Adamson, *J. Polym. Sci.*; *Part B: Polym. Phys.*, **38**, 2564 (2000).

(8) D. Pavia, *Introduction to Spectroscopy*, Thomson Learning, 2001.

(9) Analysis of the SAXS pattern was performed on the basis of the following equation: $q^2/(2\pi)^2 = h^2/(a\sin\gamma)^2 - 2hk\cos\gamma/ab\sin^2\gamma + k^2/(b\sin\gamma)^2$, where h and k are Miller indices of the scattering planes, a and b are unit cell basis vectors, and γ is the angle between a and b ($0^o < \gamma < 180^o$).

(10) V. Balsamo, F. von Gyldenfeldt, and R. Stadler, *Macromolecules*, **32**, 1226 (1999).